Experimental and computational aerodynamic characterisation of urban trees

Reference:
Koch Kyra, Samson Roeland, Denys Siegfried.- Experimental and computational aerodynamic characterisation of urban trees
Biosystems engineering - ISSN 1537-5110 - 190(2020), p. 47-57
Full text (Publisher's DOI): https://doi.org/10.1016/J.BIOSYSTEMSENG.2019.11.020
To cite this reference: https://hdl.handle.net/10067/1648830151162165141

Experimental and computational aerodynamic characterisation of urban trees

Kyra Koch[a,*], Roeland Samson[a], Siegfried Denys[b]

[*]: corresponding author, e-mail: kyra.koch@uantwerpen.be, T: +32 3 265 35 69
[a]: Research group ENdEMIC, Department of Bioscience Engineering, University of Antwerp, Groenenborgerlaan 171 2020 Antwerp, Belgium
[b]: Research group DuEL, Department of Bioscience Engineering, University of Antwerp, Groenenborgerlaan 171 2020 Antwerp, Belgium

ABSTRACT

The Darcy-Forchheimer method is used for modelling the airflow through vegetation. Seven tree and shrub species with contrasting leaf morphologies were installed in a wind tunnel to allow pressure loss measurements across the plant section. Aerodynamic parameters derived from this experiment were inserted into a COMSOL Multiphysics computational fluid dynamics model. The model was confirmed to be a good predictor for airflow through vegetation (R^2 = 0.98), regardless of plant morphology. Moreover, supplementing these data with results from a previous study (which considered herbaceous species) revealed a pattern of pressure loss data, that was already been normalised for plant area density. Although we propose further research into kinetic energy transfer in vegetation, this study provides sufficient interesting information for further applications and modelling to describe and predict urban ecology.

NOMENCLATURE

A	Area	m^2
FLS	Functional leaf size	(-)
K	Permeability	m^2
K_1	Inertial permeability	m
LAD	Leaf area density	$m^2\ m^{-3}$
LDI	Leaf dissection index	(-)
LS	Leaf size	m^2
M	Mass	kg
P	Perimeter	m
PAD	Plant area density	$m^2\ m^{-3}$
Q	Flow rate	$m^3\ s^{-1}$
R^2	Coefficient of determination	(-)
SLA	Specific leaf area	$m^2\ kg^{-1}$
q	Flux	$m\ s^{-1}$
v	Fluid velocity	$m\ s^{-1}$
V	Volume	m^3
ΔP	Pressure loss	Pa
ΔP_{norm}	Normalised pressure loss	(-)
Δx	Distance	m
ρ	Density	$kg\ m^{-3}$
φ	Porosity	(-)
τ	Kendall rank correlation coefficient	(-)
μ	Viscosity	Pa s

1 INTRODUCTION

Describing how air flows through vegetation has been proven to be challenging. However, this knowledge is indispensable in order to evaluate complex processes performed by plants such as particulate matter (PM) mitigation (Beckett et al. 1998; Nowak et al. 2006; Litschike & Kuttler 2008; Pugh et al. 2012; Samson et al. in Pearlmutter et al. 2017) and cooling effects. Furthermore, urban green infrastructure has other important functions; e.g. carbon sequestration (Tallis et al., 2015), improvement of biodiversity (Oberndorfer et al., 2007); water purification and management (Pearlmutter et al., 2017) and human wellbeing (Hartig, Mitchell, Vries, & Frumkin, 2014).

Parameterisation of aerodynamic effects of vegetation can be approached in different ways, as discussed in the review of Buccolieri et al. (2018). For example, Buccolieri et al. (2009) and Jeanjean et al. (2016) use a pressure loss coefficient λ which accounts for the ratio of the static pressure difference between the front and the back of the porous medium, and the dynamic pressure (ρ v^2) divided by the stream wise length of the material. In contrast, Koch, Samson, & Denys (2019) used the pressure drop normalized for vegetation density, wind speed and length of the material as a measure of how easily air flows throughout a certain vegetation stand. Because of different approaches involved, comparisons between studies are often difficult (Janhäll, 2015).

Aerodynamic studies of trees have often involved synthetic simulators, wire constructions or other porous media (Buccolieri et al. 2009; Endalew et al. 2009; Gromke & Ruck 2012); only a few studies have used real trees or branches (Molina-Aiz et al. 2006; Lin & Khlystov 2012; Sase, Kacira, Boulard, & Okushima, 2012; Huang et al. 2013). Moreover, several modelling approaches have been performed, which include numerical airflow models (Connell, Endalew, & Verboven, 2011; De Maerschalck, Maiheu, Janssen, & Vankerkom, 2010; Endalew et al., 2009; Hong et al., 2012) or empirical models (Raupach, Woods, Dorr, Leys, & Cleugh, 2001; Tiwary, Morvan, & Colls, 2005; M. Lin, Katul, & Khlystov, 2012b). In all of these approaches, be they experimental or modelling, simplifications are made for the sake of convenience. According to Janhäll (2015), this downscaling of vegetation increases the uncertainty of the results. Also, for trees, Jeanjean et al. (2016) have found that aerodynamic effects are more important for PM mitigation than the deposition processes themselves. This highlights the importance of aerodynamic assessment of vegetation and trees in particular.

In our earlier work, Koch et al. (2019), a Darcy-Forchheimer approach was proposed as a model to describe pressure drop over several contrasting herbaceous plant species which were considered as porous media. The Darcy-Forchheimer equation is an extension of the simple Darcy equation, which relates the pressure drop observed when a fluid flows through a porous medium to the flow rate of the fluid. The Forchheimer-drag includes inertial effects that occur at high flow rates. Freshly cut vegetation was brought into a wind tunnel setup, while pressure data results were validated in a COMSOL Multiphysics CFD (Computational Fluid Dynamics) model. Close agreement was found between experimental and modelled data, which suggests Darcy-Forchheimer as a useful approach to aerodynamically characterize different plant species for green wall applications. Furthermore, a classification of species was made in terms of their normalised pressure drop. In this paper, this approach is expanded by assessing its applicability on woody plant species. Trees and shrubs are important forms of urban green infrastructure and are different from green walls in terms of their woody mass. Leaves of trees and shrubs are growing on branches instead of on non-woody stems as with herbaceous species.

The objectives of this research are (1) to observe if the Darcy-Forchheimer approach is applicable for multiple types of vegetation; (2) to investigate potential differences between species in aerodynamic properties and to compare them with herbaceous outcomes; and (3) to examine if pressure losses over woody species can be predicted by their leaf morphology.

2 MATERIALS & METHODS

2.1 SPECIES SELECTION AND MORPHOLOGICAL PARAMETERS

Species were selected with the aim of covering a broad variety in leaf morphology. Five deciduous as well as two coniferous tree and shrub species, which are commonly found in Western Europe, were used (Table 1). Tree and shrub specimens were grown in a common garden at Groenenborger Campus of Antwerp University, Belgium. For this research, plants were selected from the same experimental setup that was used as in Muhammad, Wuyts, & Samson (2019). The plants were three years old at the time of sampling. Branches with leaves were sampled between October 2017 and January 2018. For practical reasons only one-year old branches were collected of the deciduous species. Following the method of Koch et al. (2019) a series of directly measurable leaf morphological parameters was assessed in order to describe the selected species on plant and leaf level. Parameters and calculations are given in Table 2.

Table 1: Selected species. Scientific name and largest measured length and width of an individual leaf or needle are given. “Largest” means the maximum measured length of a leaf out of all the measured leaves for the considered plant species.

Catalpa bignonioides Length x width: 200 x 150 mm	*Buddleja davidii* Length x width: 140 x 60 mm	*Betula pendula* Length x width: 40 x 60 mm	*Carpinus betulus* Length x width: 85 x 45 mm
			
Ligustrum ovalifolium Length x width: 45 x 20 mm	*Thuja plicata* Length x width: 25 x 3 mm	*Abies fraserii* Length x width: 20 x 3 mm	
			

Table 2: Morphological canopy and leaf parameters determined on the selected tree species. V_{total}: total volume of the system, V_{plant}: volume of the foliage, Al_{eaf}: total area of all the leaves, A_{plant}: area of the entire plant (leaves and stem/branches), P: leaf perimeter (m), M: dry leaf mass (kg). Circle is the largest circle that can be drawn onto a leaf.

Parameter	Formula	Unit
Plant Area Density (PAD)	$PAD = \frac{A_{plant}}{V_{total}}$	m² m^{-3}
Porosity (φ)	$\varphi = 1 - \left(\frac{V_{plant}}{V_{total}}\right)$	dimensionless
Specific Leaf Area (SLA)	$SLA = \frac{A_{leaf}}{M_{leaf}}$	m² kg^{-1}
Leaf Dissection Index (LDI)	$LDI = \frac{P_{leaf}}{\sqrt{A_{leaf}}}$	dimensionless
Functional Leaf Size (FLS)	$FLS = \frac{A_{circle}}{A_{leaf}}$	dimensionless
Leaf Size (LS)	A_{leaf}	m²

2.2 AERODYNAMIC PARAMETERS

Permeability, Forchheimer-drag and porosity are the parameters which are used in this study to define air flow through a porous medium and are derived from wind tunnel experiments. The permeability of a porous material is its ability to allow a fluid to pass through it and it is closely related to its structure and porosity. Porosity is a fraction of the volume of voids over the total volume, ranging between 0 (full) and 1 (empty). The Forchheimer-drag coefficient accounts for the kinetic energy and inertia of the fluid and the typical non-linear relation of fluid flow rate and the pressure drop (Mattis *et al.* 2012). The value of PAD and porosity, defined in Table 2, varies depending on the packing density (even for a certain species), which makes a statistical correlation analysis possible.

In order to obtain pressure loss (ΔP) data, wind tunnel experiments were performed according to the method used in Koch et al. (2019). A closed circuit wind tunnel with a total length of 6m (2m in length, 1m wide) was used with an interior fan and had an inner diameter of 103 mm (Fig. 1). On the long side there was a removable plant compartment with inner diameter 114 mm. The step change in diameter was considered in the model. Furthermore, the measured pressures and velocities were compared with model values at corresponding locations. For each wind tunnel run, the wind tunnel fan was used in three different settings; maximum (a), median (b) and minimum power (c). For each setting fan curves were derived from pressure versus flow rate values and used as a single boundary condition in the model (see further). Air velocity data was retrieved with a hot wire anemometer (CTV 110, KIMO Instruments, Chevry-Cossigny, France), which was placed ±150 mm in front of the plant compartment. Because wind speed could only be measured at one point at a time, prior to experiment execution (thus without vegetation), measurements were taken at three distances (50 mm, 25 mm and at the duct wall) from the duct wall so that average velocity could be calculated by integrating the wind profile measurements over the flow cross section. All further calculations were performed with integrated velocity data. Branches of the selected species were brought into the plant compartment as homogeneously as possible and pressure loss over the vegetation (branches with leaves attached) was derived by a Pressure Module (750PD2, FLUKE

Corporation, Gent, Belgium) with a range of ± 7 kPa and an uncertainty of 0.15%, and a Pressure Calibrator (717 30G, FLUKE Corporation, Gent, Belgium). Per tree species 6 to 8 samples with different PAD's (plant area density, Fig. 2 left panel) and corresponding porosities (Fig. 2 right panel) were examined under the three fan settings (a, b and c). Empty wind tunnel runs were performed as a reference.

Pressure loss data was used for calculation of permeability (K) [m²] and Forchheimer-drag ($\frac{\rho}{K_1}$) [kg m^{-4}] according to Koch et al. (2019) using Darcy-Forchheimer's law:

$$\frac{\Delta P}{\Delta x} = -\left(\frac{\mu}{K}\right) q - \left(\frac{\rho}{K_1}\right) q^2 \qquad \text{(Eq. 1)}$$

where Δx is the stream wise depth of the vegetation, μ the viscosity of the fluid (Pa s), ρ the fluid density (kg m^{-3}), K_1 is the inertial permeability (m) and q the fluid flux (m/s), calculated as:

$$q = v\ \varphi \qquad \text{(Eq. 2)}$$

where v is the surface averaged wind speed in the duct (m s^{-1}) and φ the porosity (dimensionless). $\frac{\rho}{K_1}$ (kg m^{-4}) is the Forchheimer-drag coefficient. The dimensionless, normalized pressure loss ΔP_{norm} was calculated from:

$$\Delta P_{norm} = \frac{\Delta P}{\rho\, v^2\, PAD\, \Delta x} \qquad \text{(Eq. 3)}$$

where ρ v² is a measure of kinetic energy per unit volume, also called the dynamic pressure (Pa).

Normalised pressure loss for modelled data was plotted and compared to similar data from Koch et al. (2019) for herbaceous green wall species.

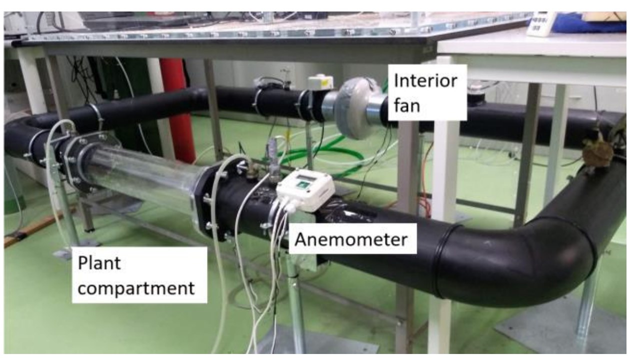

Fig. 1: Wind tunnel setup

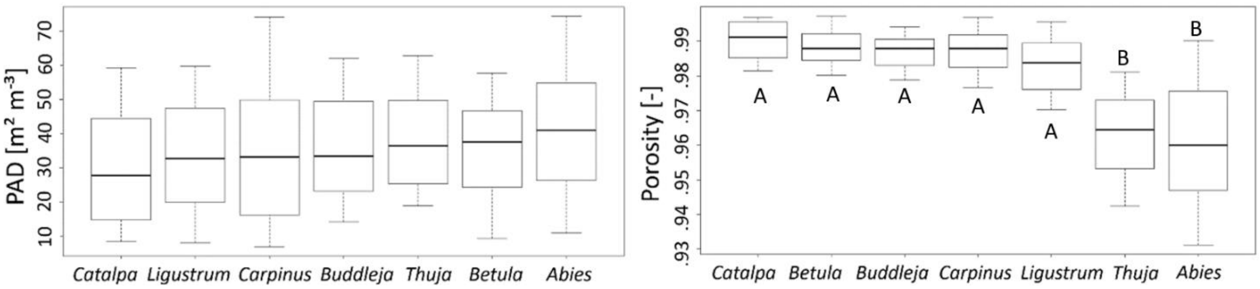

Fig. 2: Left panel: Plant Area Density (PAD [m² m^{-3}]) values for each wind tunnel run per species. There are no significant differences in densities between species. Right panel: Porosity [-] values for each species. Significant differences are indicated with the letters A-B. Error bars represent minimum and maximum values.

2.3 CFD-MODEL

For all tree species, a CFD model was developed in COMSOL Multiphysics® version 5.2a (COMSOL Inc., MA, USA), based on porosity, permeability and Forchheimer-drag derived from the wind tunnel experiment. The geometry of the entire wind tunnel was applied as in Koch et al. (2019). The plant compartment was slightly wider than the other ducts. Considering the symmetry of the geometry, only half of the geometry was meshed as shown in Fig. 3. The computational grid consisted of approximately 170,000 tetrahedral cells with refinement at the boundaries. Grid size independency was ensured by gradually refining the mesh until further refinement did not affect the results. In this case, the average mesh quality of the geometry was 0.72. A relative tolerance of 0.0001 was used as convergence criterion. Only converged solutions were considered. Physics in the wind tunnel ducts were described as turbulent flow (k-ω incompressible flow at standard conditions [101325 Pa, 293.15 K]). In contrast to the laminar flow model, the k-ω model solves for extra variables: the turbulence kinetic energy and the rate of dissipation of turbulence kinetic energy ω. A steady-state solution was generated with a direct stationary solver (relative tolerance 0.001), by solving the governing equations of momentum and mass continuity in the wind tunnel ducts (Comsol 2017):

$$\rho(\mathbf{u} \cdot \nabla)\mathbf{u} = \nabla \cdot \left(-\mathrm{P}\mathbf{I} + (\mu + \mu_T)(\nabla\mathbf{u} + (\nabla\mathbf{u})^{\boldsymbol{T}})\right) \qquad \text{(Eq. 4)}$$

$$\rho\nabla(\mathbf{u}) = \mathbf{0} \qquad \text{(Eq. 5)}$$

With ρ the air density (1.2044 kg m^{-3}), $\mathbf{u}$ the velocity vector (m s^{-1}), $\mathbf{I}$ an identity matrix, P the pressure (Pa), μ the dynamic viscosity (Pa s) and μ_T the eddy viscosity (Pa s), which is calculated by the k-ω model for a turbulent flow and equals zero in the case of a laminar flow. Second order discretisation was set by default in all equations.

For the plant compartment, Brinkman equations including Forchheimer-drag were applied (Eq. 1). As earlier research suggested these physics are the most suitable for determining air flow through vegetation (Molina-Aiz et al. 2006). To couple these two processes, pressures at the boundaries between the air ducts and the plant compartment were equalized. In Comsol, one can apply different physical processes (eg.

Brinkman's Law, turbulent air flow, …) to different domains. In order to couple the physics at neighbouring domains, boundary conditions should be defined and variables should be equal in order to connect the different domains. This is a convenient and computationally profitable approximation for single phase fluid flow in a porous medium (Bejan, 2013). A no slip condition was assumed at the walls. As mentioned earlier, the static pressure curve of the fan was used as a single boundary condition. This means that the model automatically finds the working point of the fan-duct system, corresponding to the pressure losses caused by the vegetation and the duct walls. If plants are present in the tunnel, the pressure losses are higher, shifting the working point of the fan more to the left of the graph (small Q and large delta P). If the tunnel is empty, pressure losses are low and the working point of the fan is on the right side of the graph. For a detailed explanation on how this works, the authors refer to Koch et al. (2019) and to the book "Fluid Mechanics: Fundamentals and applications, 4th edition". This means that the wind speed measured in the experiment can later be used as a validation parameter, by comparing it with the modelled wind speed. The same applies to the pressure loss measured by the pressure module and the modelled pressure loss. The pressure losses, obtained by the model, were then compared with the experimentally measured values to test the method.

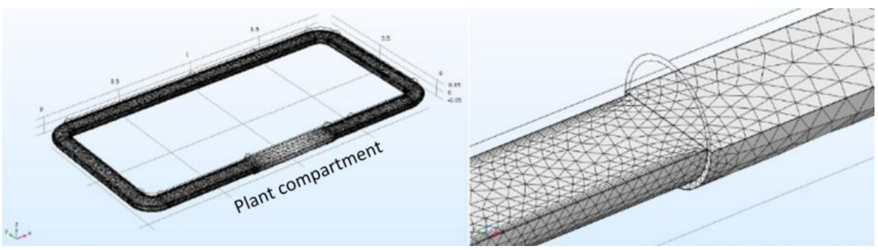

Fig. 3: Geometry of the wind tunnel (left) and the computational mesh used in the model (right)

2.4 STATISTICAL ANALYSIS

All analyses were performed in R version 3.3.1 (https://cran.r-project.org/) and using an Excel worksheet. Significance levels are always at 5%. An analysis of variance (ANOVA) was used to indicate significant differences between species and their morphological parameters. Differences were indicated by a TukeyHSD test which can be used to find means that are significantly different from each other. For permeability and Forchheimer-drag, a log transformation was performed on the data because it was skewed. To test whether permeability and Forchheimer-drag are normally distributed, a Shapiro-Wilk was used. Both parameters scored high on the test (permeability: $W = 0.97691$, p-value $= 0.01551$; Forchheimer-drag: $W = 0.95474$, p-value $= 0.0001169$), confirming a normal distribution. An ANOVA was executed to look at the differences between the species and their permeability and Forchheimer-drag. Differences were indicated by a Tukey-HSD test. Kendall rank correlations were performed to test the correlations between permeability and Forchheimer-drag and PAD and porosity. Species morphological parameters were compared with mean and median permeability and Forchheimer-drag by using ANOVA's. Another ANOVA was performed to look at the differences between normalised pressure drops, together with a Tukey-HSD to indicate the differences. Furthermore, to indicate differences between mean normalized pressure drops and plant morphological parameters, an ANOVA was used.

3 RESULTS

3.1 SPECIES MORPHOLOGY

Table 3 shows an overview of all species morphological parameters and their standard deviations. An ANOVA indicated that FLS and LDI are negatively correlated (p = 0.03994). No other correlation between morphological parameters was found.

Table 3: Mean values of Functional Leaf Size (FLS), Leaf Dissection Index (LDI), Specific Leaf Area (SLA) and Leaf Size (LS) and their standard deviations (stdev) for the considered tree and shrub species. Species that significantly differ within a parameter are indicated by different letters a – f.

Species	**mean FLS (-)**	**stdev FLS**	**mean LDI (-)**	**stdev LDI**	**mean SLA ($m^2\ kg^{-1}$)**	**stdev SLA**	**LS (m^2)**	**stdev LS**
Abies	1.15E-01 (d)	1.96E-02	7.38E+00 (a)	4.50E-01	4.72E+00 (e)	7.25E-16	2.47E-05 (d)	8.80E-06
Betula	7.50E-01 (a)	2.73E-02	5.50E+00 (a)	3.95E-01	1.08E+01 (d)	1.47E-01	1.00E-03 (bcd)	3.65E-04
Buddleja	3.76E-01 (c)	1.24E-01	5.81E+00 (a)	5.05E-01	2.14E+01 (a)	5.83E-01	1.83E-03 (bc)	1.76E-03
Carpinus	7.14E-01 (ab)	1.58E-01	5.65E+00 (a)	1.63E-01	1.33E+01 (b)	2.35E-01	1.59E-03 (bc)	7.45E-04
Catalpa	7.11E-01 (ab)	7.50E-02	4.69E+00 (a)	5.39E-01	1.26E+01 (c)	8.34E-01	1.02E-02 (a)	6.62E-03
Ligustrum	5.67E-01 (b)	9.49E-02	4.91E+00 (a)	3.27E-01	1.04E+01 (d)	3.61E-01	3.27E-04 (cd)	2.26E-04
Thuja	5.68E-02 (d)	4.74E-02	1.37E+01 (b)	3.81E+00	3.95E+00 (f)	8.55E-02	4.13E-04 (ab)	2.09E-04

3.2 AERODYNAMIC CHARACTERISATION USING WIND TUNNEL EXPERIMENTS

Permeability and Forchheimer-drag varied from 3.09×10^{-7} to 4.32×10^{-5} m^2 and from 0.42 to 41.94 kg m^{-4}, respectively. Differences in permeability are shown in Fig. 4. The ANOVA showed a significance of p = 3.138e-11. No significant differences between species in Forchheimer-drag data were found (p = 0.3571).

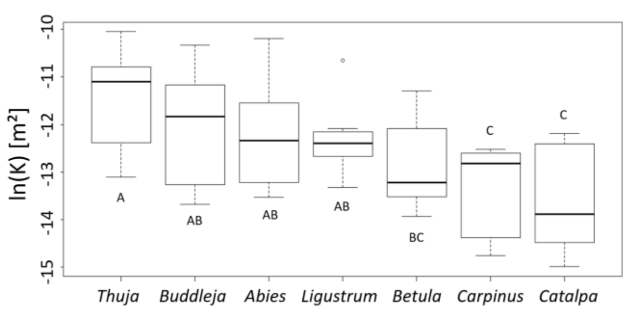

Fig. 4: Spread of permeability (natural log) values per species, classified from high to low median permeability. Significant differences are indicated with different letters A-C.

Kendall rank correlations are shown in Fig. 5. Permeability and Forchheimer-drag are strongly negatively correlated and PAD and porosity also. Both permeability and Forchheimer-drag are strongly correlated with PAD. Permeability is weakly positively correlated with porosity, while Forchheimer-drag is negatively correlated with porosity. Table 4 shows corresponding τ- and p-values and equations of the trend lines.

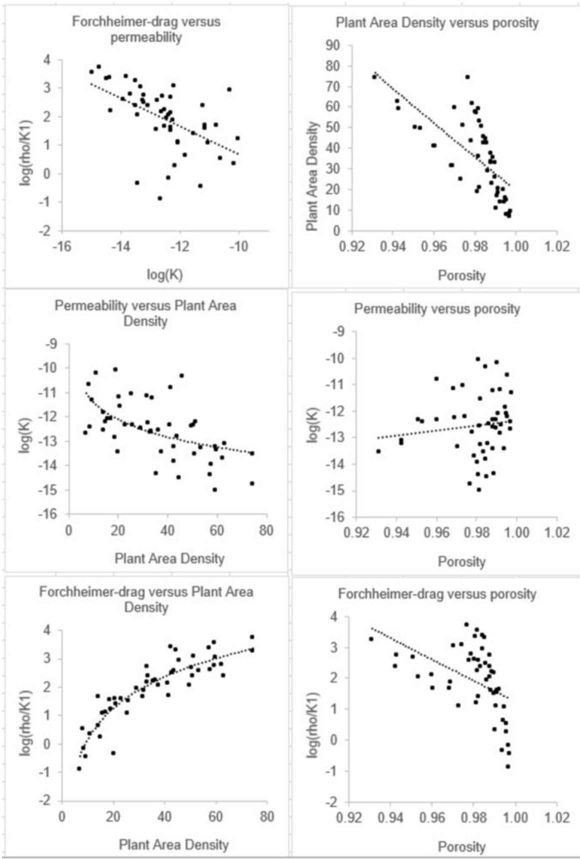

Fig. 5: Kendall rank correlations between permeability (K, m^2), Forchheimer-drag (kg m^{-4}), plant area density (m^2 m^{-3}) and porosity (-). Each points represents one wind tunnel run for a specific species under different wind speeds. Trend lines are also given (dotted line). Tau-values, p-values and equations of the trend lines are given in accessory table x.

Table 4: Accessory to Figure x: tau-values, p-values and equations of the trend lines shown in Fig. 4.

Forchheimer-drag versus permeability	Plant Area Density versus porosity
τ = -0.4698582 p = < 2.2e-16 y = -0.4924x - 4.252	τ = 0.3187921 p = 2.548e-08 y = -795.3ln(x) + 19.764
Permeability versus Plant Area Density	Permeability versus porosity
τ = -0.3546099 p = 4.93e-10 y = -1.033ln(x) - 9.0109	τ = 0.137134 p = 0.01657 y = 9.7566x - 22.098
Forchheimer-drag versus Plant Area Density	Forchheimer-drag versus porosity
τ = 0.09751773 p = 0.08711 y = 1.5974ln(x) - 3.5284	τ = -0.4719548 p = < 2.2e-16 y = -33.14ln(x) + 1.2526

3.3 CORRELATION BETWEEN AERODYNAMIC AND MORPHOLOGICAL PARAMETERS

Correlations between mean and median permeability and Forchheimer-drag and the morphological parameters are given in Table 5. Table 5 shows that the variance in mean permeability can be explained by FLS and the variance in median permeability can be explained by LDI. Correlations are plotted in Figure 6.

Table 5: Morphological parameters Specific Leaf Area (SLA), Leaf Dissection Index (LDI), Functional Leaf Size (FLS) and Leaf Size (LS) as a function of permeability (K) and Forchheimer-drag (ρ/K_1). P-values of the correlations as result of an ANOVA are given. Stars indicate significant p-values (p =< 0.05).

	Mean K	**Mean ρ/K_1**	**Median K**	**Median ρ/K_1**
SLA (m^2 kg^{-1})	0.47	0.45	0.48	0.29
LDI (-)	0.02 *	0.20	0.0034 *	0.41
FLS (-)	0.0051 *	0.25	0.034 *	0.46
LS (m^2)	0.27	0.57	0.36	0.45

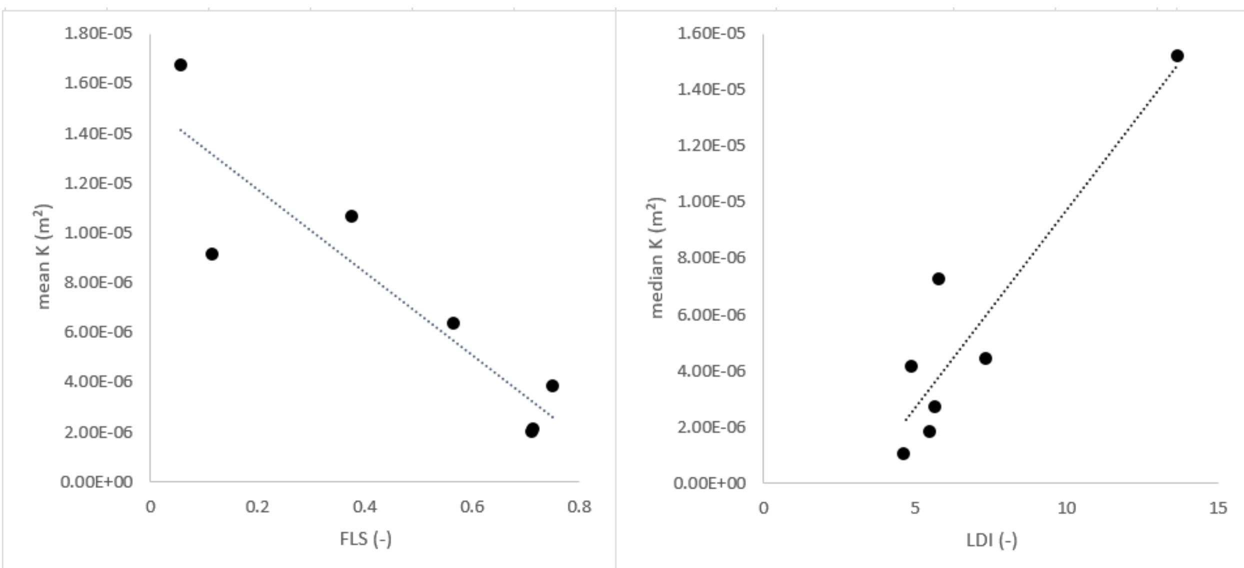

Fig. 6: Left: The correlation between Functional Leaf Size (FLS) (-) and the mean values for permeability K (m^2). Equation of trend line: $y = -1.66 \cdot 10^{-5} x + 1.50 \cdot 10^{-5}$. Right: The correlation between Leaf Dissection Index (LDI) (-) and median values for permeability K (m^2). Equation of trend line: $y = 10^{-6} x + 4 \cdot 10^{-6}$. Each point represents a species. Trend lines are shown as dotted lines. R^2 values of the trend lines are 0.82 (left) and 0.85 (right).

3.4 CFD-MODEL

Fan curves were derived from wind tunnel runs on three different fan power settings (see section 2.2). In Koch et al. (2019) the same was done on five different power settings (a to e) and results of both tests are given in Fig. 7. A typical result from the CFD model is given in Fig. 8. Other runs showed similar results.

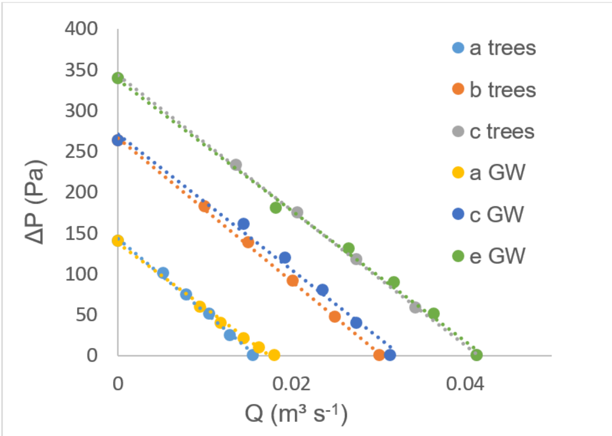

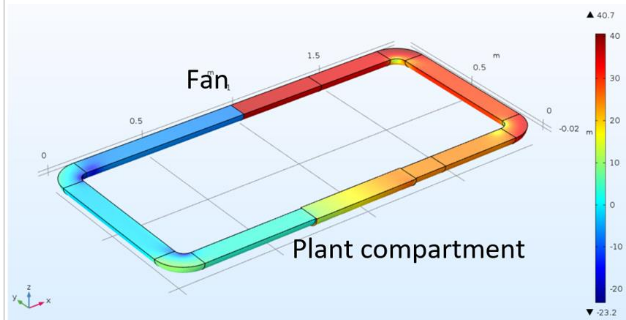

Fig. 7: Fan curve derived from trees (this paper) for three settings (a [low],b [middle] and c [high]) compared to fan curve derivation from Koch et al. (2018) for herbaceous green wall [GW] species (settings a, c and e).

Fig. 8: Typical pressure distribution obtained by the CFD model for the specific case of *Catalpa* (PAD = 14.80 (m^2 m^{-3}), φ = 0.9955, K = 5.0907*10^{-6}, ρ/K1 = 1.3007 kg m^{-4})

The model was validated by plotting the measured average wind speed over the cross-section of the tunnel by the anemometer against the simulated wind speed at the exact position of the anemometer (Fig. 9 left panel), also integrated and averaged over the cross-section of the tunnel. Given that the fan was the only boundary condition (see section 2.2), this is a reliable method. A good agreement between model and experiment was found (R^2 = 0.98). The same applies to pressure loss data, as the modelled pressure loss corresponds well to experimental pressure loss (Fig. 9 right panel).

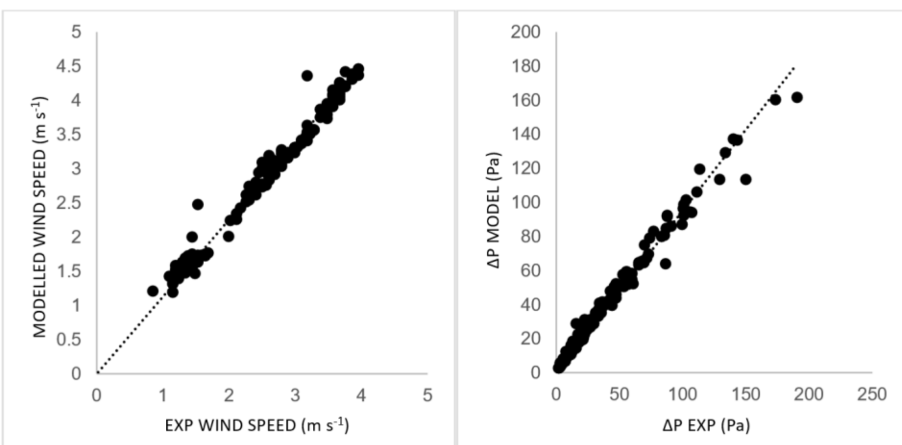

Fig. 9: Scatter plot of all experimental versus modelled data. Each dot represents a specific wind tunnel run. The dotted lines represent the trend lines. Left panel: relationship between measured (exp) and modelled wind speed. Equation: y = 1.1284x, R^2 = 0.98. Right panel: modelled versus experimental pressure loss (ΔP). Equation: y = 0.95x, R^2 = 0.98.

Figure 10 shows a ranking for normalized pressure losses (ΔP_{norm}) of the considered tree species supplemented with data from Koch et al. (2019) on herbaceous green wall species. Because of the good correlation of experimental and modelled pressure losses (Fig. 9 right panel), only modelled values are shown. Even though a normalization for air and plant density, wind speed and stream wise depth of the plant compartment was performed (Eq. 3), clear differences can be seen between species and significantly different groups (p-value of < $2.2 \cdot 10^{-16}$) can be distinguished (A-E). The first group consists of five species (*Thuja, Abies, Buddleja, Ligustrum, Betula* and *Festuca*), while e. g. *Catalpa* and *Carpinus* have clearly much higher values. The figure shows that in general tree species have a lower score for ΔP_{norm} values, as well as a smaller range, where herbaceous species have higher values and wider ranges for normalised pressure drop. For every species a mean normalised pressure loss was calculated for modelled values in order to test against morphological parameters. An ANOVA showed that no variance in normalised pressure loss could be explained by either one of the considered morphological parameters on their own or by interactions.

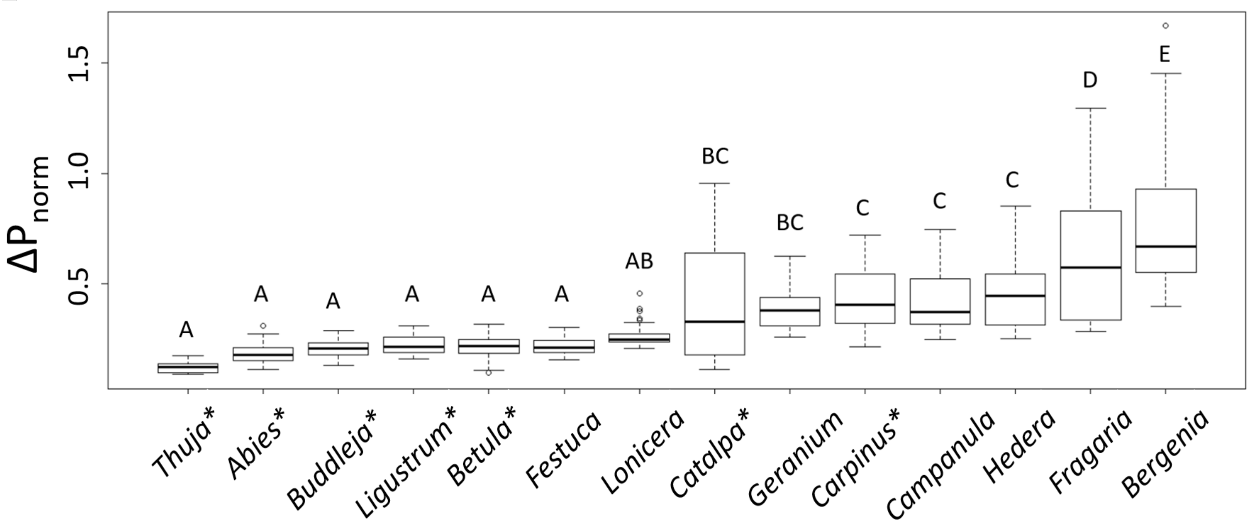

Fig. 10: Normalised pressure losses for tree and shrub species used in this paper (indicated with a *) and for herbaceous green wall species as reported in Koch et al. (2019). Significant differences are indicated with the letters A-E.

4 DISCUSSION

4.1 WIND TUNNEL EXPERIMENTS

In general, wind tunnel studies are convenient because several environmental variables can be controlled, which makes it interesting for providing data for validating model simulations. Moreover, in the case of this research, edge effects of airflow on a vegetation stand are minimalized, because the wind tunnel is entirely filled, and air is forced to go through the vegetation. In contrast, most wind tunnel studies describe airflow around vegetation, where other flow patterns occur.

Tree and shrub branches of different porosities, ranging from 93.1% (*Abies*) to 99.7% (*Betula*) (Fig. 2 right panel) were brought into the wind tunnel. This is a wider range than Gromke & Ruck (2012), who found porosities of 96 to 97.5%. Lin et al. (2012) found in a similar experiment with variable packing densities (volume vegetation/volume wind tunnel) of 0.037 and 0.055 for Juniper and 0.017 and 0.040 for Pine. Our packing densities varied in a wider range, from 0.002 (*Betula*) to 0.069 (*Abies*). In addition, earlier research within the department showed values for permeability and Forchheimer-drag of 3.8×10^{-7} m^2 and 29 kg m^{-4}, respectively and a porosity above 99% for fiberglass. These values fall into the range of this study (permeability from 3.1×10^{-7} to 4.3×10^{-5} m² and Forchheimer-drag from 0.4 to 41.9 kg m^{-4}), which implies that fiberglass could be deployed to simulate certain plant species. Similarly to the findings of Koch et al. (2019), permeability seemed to be influenced by species (Fig. 4), but Forchheimer-drag did not, even though roughly the same ranges of densities (Fig. 2 left panel) were used per species. The differences in permeability could partially be explained by some leaf morphological parameters, namely FLS and LDI, which had a negative and positive correlation with mean permeability and median permeability, respectively (Fig. 6). This means that permeability can be (partially) predicted by looking at a species' leaf shape, more specifically its degree of roundness and serration. These results are different from, but not contradictory to the findings in Koch et al. (2019), where correlations between permeability and SLA, and Forchheimer-drag and FLS were found.

Figure 5 (centre, left) shows a logical agreement between permeability and PAD, as more plant material is less penetrable by air. This is in accordance to Sase et al. (2012). It also shows a correlation of permeability with Forchheimer-drag (Fig. 5 top, left), which means Forchheimer-drag can be estimated from permeability data. Furthermore, a correlation was found between Forchheimer-drag and PAD (Fig. 5 bottom, left). This indicates that by considering only plant density, the Forchheimer-drag can be estimated. This correlation is also logical because more plant material means more air flow being blocked, which results in higher turbulence and inertia. Figure 5, top right, shows a negative correlation of PAD and porosity. This makes sense, since both parameters are related to the amount of plant material present, but in an opposite way. Porosity and permeability are positively related since the presence of more void spaces facilitates the air flow through the vegetation. On the other hand, Forchheimer-drag has a strong negative correlation with porosity, which indicates that drag forces are more important when the vegetation is packed more densely.

4.2 MODEL VS. EXPERIMENT

In general, CFD models provide a fast, cheap and easy way to assess physical processes. They can be used on micro- or full scale and are able to rule out environmental variables which can make it difficult to compare experiments, such as meteorological conditions. Figure 9 (right panel) shows a good correlation between modelled and experimental pressure drops, which means that the Darcy-Forchheimer model is a good proxy for what happens with wind flow through vegetation for woody species that are considered as trees and shrubs. Consequently, it is safe to assume this model works for a wide diversity of woody and herbaceous plant species. Validation with wind speed also indicates a good fit between model and experiment.

After normalization for air and plant density, wind speed and stream wise plant depth, a clear pattern in pressure losses could be found between species (Fig. 10). This would be expected to be caused by species-specific morphological characteristics. Nevertheless, even after addition of data from Koch et al. (2019), no correlations with the considered morphological parameters could be found. Because of these findings, we assume that the transfer of impulse is an important factor influencing the pressure loss. Depending on the rigidity of the vegetation structures, wind energy is partially converted into branch and leaf movement, resulting in an additional pressure loss that was not considered in the study. It was clearly observed that there were vibrations of leaves and thin branches during the experiments, even at the lowest air speed. Investigating the effect of rigidity would demand experiments to be performed at even lower air speeds, which was not possible with the equipment used. Also, rigidity or stiffness tests of the vegetation material should be conducted using a stiffness tester or similar device. We believe that such research would lead to important new insights on the aerodynamics of vegetation. In a rigorous approach, leaves and branches can be considered as multiple masses connected by springs and dampers, where also rotational inertia is involved.

It is therefore proposed that further research should include the transfer of impulse, along with the Navier-Stokes equations and the transfer of energy to heat due to viscous effects. This is a challenging task as the transfer of impulse depends on other parameters that were not considered in this work, for example the rigidity of the vegetation structures. However, plant permeability can be (partly) predicted by assessing a species' leaf shape, more specifically LDI and FLS. On the other hand, PAD was found to be a determining factor for Forchheimer-drag.

5 CONCLUSIONS

This study suggests that the Darcy-Forchheimer approach works for describing air flow through multiple types of vegetation. Consequently, it can be used for modelling the interactions between atmosphere and environment and contribute to a wider knowledge on this topic. The Darcy-Forchheimer approach can be considered a holistic approach because it covers the integrated effect of leaves, stems, branches and their size, shape, density and rigidity.

Moreover, plant species can be classified under a range of pressure drops normalised for density. In other words, there is a difference in normalised pressure drop between species that cannot be explained by the used leaf morphological parameters. It is proposed that further research into kinetic energy transfer based on rigidity factor is carried out. However, plant permeability can be (partly) predicted by assessing a species' leaf shape, more specifically LDI and FLS and PAD was found to be a determining factor for Forchheimer-drag.

ACKNOWLEDGEMENTS

This work was supported by the VLAIO-VIS project 'Green building: green walls for sustainable buildings and cities' (140993) and the FWO-SBO project 'EcoCities: Green roofs and walls as a source for ecosystem services in future cities' (S002818N).

REFERENCES

Beckett, K. P., Freer-Smith, P. H., & Taylor, G. (1998). Urban woodlands: Their role in reducing the effects of particulate pollution. *Environmental Pollution*, *99*(3), 347–360. https://doi.org/10.1016/S0269-

7491(98)00016-5

Bejan, A. (2013). Convection Heath Transfer. 4th ed. City: John Wiley & Sons, Inc., 658p., pages 537-605. Available at: http://onlinelibrary.wiley.com/book/10.1002/9781118671627.

Buccolieri, R., Gromke, C., Di Sabatino, S., & Ruck, B. (2009). Aerodynamic effects of trees on pollutant concentration in street canyons. *Science of the Total Environment*, *407*(19), 5247–5256. https://doi.org/10.1016/j.scitotenv.2009.06.016

Buccolieri, R., Santiago, J. L., Rivas, E., & Sanchez, B. (2018). Review on urban tree modelling in CFD simulations: Aerodynamic, deposition and thermal effects. *Urban Forestry and Urban Greening*, *31*(March), 212–220. https://doi.org/10.1016/j.ufug.2018.03.003

çengel and Cimbala (2018). Fluid Mechanics: Fundamentals and applications. 4th ed. Mc Graw Hill,

Connell, R. J., Endalew, a M., & Verboven, P. (2011). CFD Modelling of Kiwifruit Vines and Leaves : A method of handling multiple thin surfaces. *19th International Congress on Modeling and Simulation*, (December), 12–16.

De Maerschalck, B., Maiheu, B., Janssen, S., & Vankerkom, J. (2010). CFD-Modelling of complex plant-atmosphere interactions: direct and indirect effects on local turbulence. *HARMO 2010 - Proceedings of the 13th International Conference on Harmonisation within Atmospheric Dispersion Modelling for Regulatory Purposes*, 839–842.

Endalew, a. M., Hertog, M., Delele, M. a., Baetens, K., Persoons, T., Baelmans, M., … Verboven, P. (2009). CFD modelling and wind tunnel validation of airflow through plant canopies using 3D canopy architecture. *International Journal of Heat and Fluid Flow*, *30*(2), 356–368. https://doi.org/10.1016/j.ijheatfluidflow.2008.12.007

Gromke, C., & Ruck, B. (2012). Pollutant Concentrations in Street Canyons of Different Aspect Ratio with Avenues of Trees for Various Wind Directions. *Boundary-Layer Meteorology*, *144*(1), 41–64. https://doi.org/10.1007/s10546-012-9703-z

Hartig, T., Mitchell, R., Vries, S. De, & Frumkin, H. (2014). Nature and Health. https://doi.org/10.1146/annurev-publhealth-032013-182443

Hong, B., Lin, B.-R., Wang, B., & Li, S.-H. (2012). Optimal design of vegetation in residential district with numerical simulation and field experiment. *Journal of Central South University of Technology (English Edition)*, *19*(3), 688–695. https://doi.org/10.1007/s11771-012-1058-6

Huang, C. W., Lin, M. Y., Khlystov, A., & Katul, G. (2013). The effects of leaf area density variation on the particle collection efficiency in the size range of ultrafine particles (UFP). *Environmental Science and Technology*, *47*(20), 11607–11615. https://doi.org/10.1021/es4013849

Janhäll, S. (2015). Review on urban vegetation and particle air pollution - Deposition and dispersion. *Atmospheric Environment*, *105*, 130–137. https://doi.org/10.1016/j.atmosenv.2015.01.052

Jeanjean, A. P. R., Monks, P. S., & Leigh, R. J. (2016). Modelling the effectiveness of urban trees and grass on PM2.5reduction via dispersion and deposition at a city scale. *Atmospheric Environment*, *147*, 1–10. https://doi.org/10.1016/j.atmosenv.2016.09.033

Koch, K., Samson, R., & Denys, S. (2019). Aerodynamic characterisation of green wall vegetation based on plant morphology: An experimental and computational fluid dynamics approach. *Biosystems Engineering*, *178*. https://doi.org/10.1016/j.biosystemseng.2018.10.019

Lin, M.-Y., & Khlystov, A. (2012). Investigation of Ultrafine Particle Deposition to Vegetation Branches in a Wind Tunnel. *Aerosol Science and Technology*, *46*(4), 465–472. https://doi.org/10.1080/02786826.2011.638346

Lin, M., Katul, G. G., & Khlystov, a. (2012). A branch scale analytical model for predicting the vegetation collection efficiency of ultrafine particles. *Atmospheric Environment*, *51*, 293–302. https://doi.org/10.1016/j.atmosenv.2012.01.004

Litschike, T., & Kuttler, W. (2008). On the reduction of urban particle concentration by vegetation - A review. *Meteorologische Zeitschrift*, *17*(3), 229–240. https://doi.org/10.1127/0941-2948/2008/0284

Mattis, S., Dawson, C., Kees, C., & Farthing, M. (2012). Numerical Modeling of Flow Through Domains With Simple Vegetation-Like Obstacles, 1–8. Retrieved from http://cmwr2012.cee.illinois.edu/Papers/Special Sessions/Multiphase and Pore-Scale Modeling - Challenges and Perspectives/Mattis.Steven.pdf

Molina-Aiz, F. D., Valera, D. L., Álvarez, A. J., & Madueño, A. (2006). A Wind Tunnel Study of Airflow through Horticultural Crops: Determination of the Drag Coefficient. *Biosystems Engineering*, *93*(4), 447–457. https://doi.org/10.1016/j.biosystemseng.2006.01.016

Muhammad, S., Wuyts, K., & Samson, R. (2019). Atmospheric net particle accumulation on 96 plant species with contrasting morphological and anatomical leaf characteristics in a common garden experiment. *Atmospheric Environment*, *202*(January 2019), 328–344. https://doi.org/10.1016/j.atmosenv.2019.01.015

Nowak, D. J., Crane, D. E., & Stevens, J. C. (2006). Air pollution removal by urban trees and shrubs in the United States. *Urban Forestry and Urban Greening*, *4*(3–4), 115–123. https://doi.org/10.1016/j.ufug.2006.01.007

Oberndorfer, E., Lundholm, J., Bass, B., Coffman, R. R., Doshi, H., Dunnett, N., … Rowe, B. (2007). Green Roofs as Urban Ecosystems: Ecological Structures, Functions, and Services. *BioScience*, *57*(10), 823–833. https://doi.org/10.1641/B571005

Pearlmutter, D., Calfapietra, C., Samson, R., O’Brien, L., Krajter, S. O., Sanesi, G., & Amo, R. A. del. (2017). *The Urban Forest: Cultivating Green Infrastructure for People and the Environment*. *Springer*. https://doi.org/10.1007/978-3-319-50280-9

Pugh, T. a M., Mackenzie, a R., Whyatt, J. D., & Hewitt, C. N. (2012). Effectiveness of green infrastructure for improvement of air quality in urban street canyons. *Environmental Science & Technology*, *46*(14), 7692–7699. https://doi.org/10.1021/es300826w

Raupach, M. R., Woods, N., Dorr, G., Leys, J. F., & Cleugh, H. A. (2001). The entrapment of particles by windbreaks. *Atmospheric Environment*, *35*(20), 3373–3383. https://doi.org/10.1016/S1352-2310(01)00139-X

S. Sase, M. Kacira, T. Boulard, & L. Okushima. (2012). Wind Tunnel Measurement of Aerodynamic Properties of a Tomato Canopy. *Transactions of the ASABE*, *55*(5), 1921–1927. https://doi.org/10.13031/2013.42354

Tallis, M. J., Amorim, J. H., Calfapietra, C., Freer-Smith, P., Grimmond, S., & Kotthaus, S. (2015). The impacts of green infrastructure on air quality and temperature. *Handbook on Green Infrastructure*, (November), 30–49. https://doi.org/10.4337/9781783474004.00008

Tiwary, A., Morvan, H. P., & Colls, J. J. (2005). Modelling the size-dependent collection efficiency of hedgerows for ambient aerosols. *Journal of Aerosol Science*, *37*(8), 990–1015. https://doi.org/10.1016/j.jaerosci.2005.07.004